

# In vivo and in vitro evaluation of $^{177}\text{Lu}$ -labeled DOTA-2-deoxy-D-glucose in mice. A novel radiopharmaceutical agent for cells imaging and therapy

Jie Zhang<sup>1,2</sup> MD,  
Zi Wang<sup>2</sup> MD,  
Huipian Liu<sup>2</sup> MD,  
Liang Cai<sup>1,2</sup> MD,  
Yue Feng<sup>2</sup> MD,  
Ling Zhou<sup>2</sup> MD,  
Hongyuan Wei<sup>2,3</sup> MD,  
Ying Xie<sup>1</sup> PhD,  
Yue Chen<sup>1,2</sup> MD

Jie Zhang and Zi Wang contribute equally to this work.

1. State Key Laboratory of Quality Research in Chinese Medicine, Macau University of Science and Technology, Taipa, Macau (SAR), PR, China.

2. Department of Nuclear Medicine, The Affiliated Hospital, Southwest Medical University, Sichuan Key Laboratory of Nuclear Medicine and Molecular Imaging, No. 25, Taiping St., Luzhou, 646000, Sichuan, PR China.

3. Institute of Nuclear Physics and Chemistry, China Academy of Engineering Physics, 621900 Mianyang, PR China; Key Laboratory of Nuclear Medicine and Molecular Imaging of Sichuan Province, 621999 Mianyang, PR China.

**Keywords:**  $^{177}\text{Lu}$ -DOTA-deoxyglucose

-Targeted radionuclide therapy  
-Cancer imaging

## Corresponding authors:

Ying Xie, PhD  
State Key Laboratory for Quality Research of Chinese Medicine, Macau University of Science and Technology, Taipa, Macau (SAR); and Yue Chen, MD  
Department of Nuclear Medicine, The Affiliated Hospital, Southwest Medical University, Sichuan Key Laboratory of Nuclear Medicine and Molecular Imaging, No. 25, Taiping St., Luzhou, 646000, Sichuan, PR China; Tel: 0830-3165722; cd03uq@163.com

Received:

9 May 2019

Accepted revised:

4 June 2019

## Abstract

**Objectives:** Incorporation of lutetium-177 ( $^{177}\text{Lu}$ ) into suitable molecules that are implicated in cancer pathology represents a promising approach for the diagnosis and treatment of cancer. The goal of the present study was to develop a novel  $^{177}\text{Lu}$  labeled radiopharmaceutical agent for both radioimaging and targeted radionuclide therapy. **Animals and Methods:** Given the synthetic versatility of 1,4,7,10-tetraazacyclododecane-1,4,7,10-tetraacetic acid (DOTA) ligand as a metal chelator and high demand of sugar molecules such as deoxyglucose (DG) in cancer cells, we carried out the radiosynthesis of a novel radiopharmaceutical agent, namely,  $^{177}\text{Lu}$ -DOTA-DG, and utilized it for imaging of cancer and also for the targeted radiation therapy of cancer tissues. **Results:** In this study, we developed an efficient radiochemical synthesis of  $^{177}\text{Lu}$ -DOTA-DG and evaluated its pharmacological properties in vitro/in vivo. Our results showed DOTA-DG can be labeled with  $^{177}\text{Lu}$  with excellent radiochemical yield at 90°C in 30min. The resulting  $^{177}\text{Lu}$ -DOTA-DG exhibited high degree of stability without significant radiolysis up to 120h in human serum and phosphate buffer. Favorable pharmacokinetics profile was demonstrated by rapid blood clearance in 4T1 murine tumor mice and heterogeneous whole body biodistribution of  $^{177}\text{Lu}$ -DOTA-DG. Further, Comet assay experiments indicated that cancer cells treated with  $^{177}\text{Lu}$ -DOTA-DG showed significant higher degree of DNA damage compared to cells treated with  $^{177}\text{Lu}^{3+}$  or non-treated cells. **Conclusion:** This study showed that there is a great potential of using  $^{177}\text{Lu}$ -DOTA-DG as an imaging and therapeutic agent for cancer diagnosis and treatment. Furthermore, this study provides valuable information for developing novel  $^{177}\text{Lu}$ -labeled radiopharmaceuticals.

Hell J Nucl Med 2019; 22(2): 103-110

Epub ahead of print: 7 July 2019

Published online: 20 July 2019

## Introduction

Targeted radionuclide therapy (TRT) has recently emerged as a powerful strategy to tackle unmet medical needs in cancer treatment [1-2]. This strategy relies on the delivery of a radiolabeled compound to specific malignant targets such as cancer cells. In contrast to traditional chemo/radiotherapy that impose undesirable threat to normal cells [3-5], the TRT is featured by targeted delivery of radioactive warhead that can emit  $\alpha$  or  $\beta$  particles directly to the tumor tissue while avoiding irradiation of healthy tissue [6]. Lutetium-177 ( $^{177}\text{Lu}$ ) has a half-life of 6.71 days and decays through  $\beta$ -particle emission and  $\gamma$  emission to a stable hafnium-177 ( $^{177}\text{Hf}$ ). The relatively long half-life helps to reduce the number of radiopharmaceutical injections to the patient, which in turn reduces the radiation dose to the patient. Given its relative long half-life and unique decay mode,  $^{177}\text{Lu}$  is useful for both radioimaging [7-8] and radiotherapy [9-13]. In particular, the average penetration of  $\beta$ -particles released by  $^{177}\text{Lu}$  in soft tissue is 670 $\mu\text{m}$ , making this radionuclide a suitable tool for delivering radiation energy within small space, including micro-metastatic disease and tumor cells near the luminal surface [14]. Therefore,  $^{177}\text{Lu}$  effectively localizes cytotoxic radiation in a relatively small area, and precisely destroys tumors smaller than 3mm in diameter, with less damage to adjacent normal tissues [15-16]. In addition to the therapeutic benefits through  $\beta$  decay, simultaneous emission of  $\gamma$  photons with appropriate energy can also be imaged to provide valuable temporal and functional information within the tumor tissues to evaluate response to treatment [17]. The utility of  $^{177}\text{Lu}$  as a radionuclide in targeted radiotherapy has long been established [18]. For example, it has been widely used in a variety of clinical trials in recent years, including prostate cancer [19], adult neuroendocrine diseases [20] and colorectal carcinoma [21] and is frequently used for peptide receptor radionuclide therapy [22].

In order to achieve the desired therapeutic and diagnostic (combined as “theranostic”)

benefits of the  $^{177}\text{Lu}$ , a judicious design of the delivering carrier and a reliable and robust linker that bridges  $^{177}\text{Lu}$  and the carrier becomes critical. Glucose is one of the three major energy sources in the human body, especially for tissues with high glucose metabolism, such as brain, kidney and cancer cells [23]. Consequently, glucose and its analogs can be exploited as suitable carrier for cancer-specific delivery. For instance, fluorine-18-labeled 2-deoxy-2-fluoro-D-glucose ( $^{18}\text{F}$ -FDG) [24] has found widespread use in positron emission tomography (PET) imaging of cancer [25] or neurodegenerative diseases [26]. However, due to intrinsic shorter half-life and single positron decay mode,  $^{18}\text{F}$ -FDG is largely limited to PET imaging and is not suitable for theranostic applications. More importantly, most sugar molecules do not comprise an appropriate labeling site to introduce metal atoms and are thus not amenable for direct  $^{177}\text{Lu}$ -labeling. As a result, a linker unit such as multi-dentate chelating ligand is necessary to bridge the radionuclide and the carrier moiety. In view of the recent development of radiolabeling strategy that involves chelation of metal-based nuclide with multidentate ligand [27–29], we envisioned that a sugar carrier could be indirectly labeled with metal nuclides through chelation chemistry. As part of our continuing efforts in developing novel sugar based radiopharmaceuticals, we recently reported the development of technetium-99m ( $^{99\text{m}}\text{Tc}$ ) labeled DTPA-DG (diethylenetriaminepentaacetic acid-DTPA, deoxy-glucosamine-DG) and rhenium-188 ( $^{188}\text{Re}$ ) labeled DTPA-DG, which demonstrated therapeutic effects in nude mice bearing breast cancer (MCF-7 cells). In addition, Lee et al. (2017) reported the successful synthesis of gallium-68 ( $^{68}\text{Ga}$ )-labeled DOTA-Capsaicin which showed high tumor to non-tumor ratios and distinct biodistribution results [30].

Inspired by previous studies, we developed a novel  $^{177}\text{Lu}$ -labeled agent, namely, 1,4,7,10-tetraazacyclododecane-1,4,7,10-tetraacetic acid (DOTA)-2-deoxy-D-glucose ( $^{177}\text{Lu}$ -DOTA-DG). In this study, we prepared  $^{177}\text{Lu}$ -DOTA-DG by chelation of  $^{177}\text{Lu}^{3+}$  with DOTA ligand, which has shown excellent stability in phosphate buffered saline buffer (PBS) and human blood serum. We were able to demonstrate in mice high binding affinity of  $^{177}\text{Lu}$ -DOTA-DG with tumor tissues through in vitro cell uptake study, whole body biodistribution study, and in vivo imaging. Furthermore, we confirmed the DNA damaging process of cancer cells induced by  $^{177}\text{Lu}$ -DOTA-DG through Comet assays. Accordingly, we present here in our efforts in exploring a novel  $^{177}\text{Lu}$ -labeled radiopharmaceutical agent for theranostic applications and this work may lead to an alternative approach for cancer diagnosis and treatment.

## Animals, Materials and Methods

### Synthesis of the labeling precursor DOTA-DG

2-deoxy-D-glucosamine hydrochloride (DG-HCl) (2.8mg, 0.13mmol) was mixed with DOTA-NHS-ester (9.1mg, 0.12mmol) in an aqueous solution (Figure 1). The resulting solution was stirred at room temperature for 48h followed by

addition of 0.01mol/L sodium bicarbonate solution to adjust the pH to 8. The progress of the reaction was monitored by high-performance liquid chromatography (HPLC). After completion of the reaction, the crude product of DOTA-DG was purified and isolated by preparative HPLC and lyophilized for the following steps. DOTA-DG was analyzed via the Waters Quadrupole Mass Spectrometer (ACQUITY QDa) system equipped with an ACQUITY UPLC BEH Amide 1.7 $\mu\text{m}$  Column (2.1 $\times$ 100mm). High-performance liquid chromatography solvent system is as follows: solvent A=0.1% trifluoroacetic acid (TFA) in acetonitrile; solvent B=0.1% TFA in water. The solvent gradient is as follows: A, 0%–85% over 0–2 min; A, 85%–65% over 2–30min; A, 65%–85% over 30–35min. The flow rate was 1mL/min.

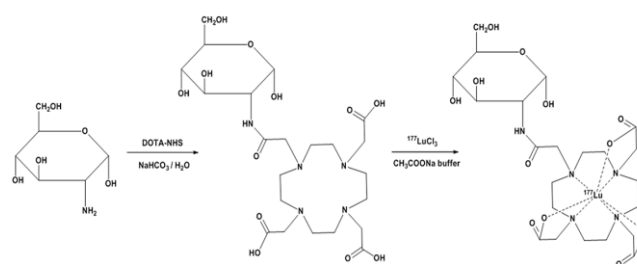


**Figure 1.** The synthesis of DOTA-DG and radiolabeling with  $^{177}\text{Lu}^{3+}$ .

### Radiolabeling of DOTA-DG with $^{177}\text{Lu}$

To optimize the conditions for the  $^{177}\text{Lu}$ -labeling of DOTA-DG, several reaction parameters including reaction time, temperature, pH and ligand concentrations were screened. The radiolabeling was performed in small volumes of sodium acetate buffer (typically 50–100 $\mu\text{L}$ ) using double-sealed plastic reaction tubes (PCR thermocycler tubes, max volume 200 $\mu\text{L}$ , BIO-RAD, USA). The pH was regulated by 1M sodium hydrogen acetate buffer solution or 1M acetic acid buffer solution. Heating was performed in a temperature-controlled heating block (Wiggins, Germany). All reactions were carried out at least in duplicate runs, using at least two different production batches of the  $^{177}\text{Lu}$  radionuclides.

### Determination of radiochemical yield (RCY)

The radiochemical yield of  $^{177}\text{Lu}$ -DOTA-DG was analyzed by radio TLC scanner (Bioscan, USA). Sheets of No. 1 Xinhua filter paper (Hangzhou Xinhua Group Co., Ltd., Hangzhou, China) were cut into 1.2 $\times$ 30cm strips. Samples of 1 $\mu\text{L}$  were applied to the strips and were developed in 10% ammonium acetate and 50% methanol mixture solution as mobile phases. The paper strips were dried thoroughly and the radioactivity was measured by radio TLC. The chromatograms were visualized using CS Chrom Plus software. The R<sub>f</sub> value of the radiolabeled  $^{177}\text{Lu}$ -DOTA-DG was 0.8 to 1.0 and R<sub>f</sub> of the free  $^{177}\text{Lu}^{3+}$  was in the range of 0 to 0.3. The error in measurements of the radiochemical conversion was approximately  $\pm 5\%$ .

### Stability studies

In vitro stability experiments were carried out according to previously published procedures [31]. The stability of  $^{177}\text{Lu}$ -DO-

TA-DG was measured in fresh human serum and PBS at 37°C. Briefly, an aliquot of 25 µL of the  $^{177}\text{Lu}$ -DOTA-DG (3.7 MBq) was added to serum or PBS and incubated at 37°C for 120h. In addition, a control experiment where the  $^{177}\text{Lu}$ -DOTA-DG was kept at room temperature in the original solution was also conducted. The radiochemical purity in different time points was monitored by radioTLC at 4h, 24h, 48h, 72h, 96h and 120h of incubation.

### In vitro cell uptake assay

4T1 murine breast cancer cells were maintained in RPMI 1640 medium (Invitrogen) supplemented with 10% fetal bovine serum and were incubated at 37°C in a 5%  $\text{CO}_2$  humidified incubator. Cell uptake assays were performed after seeding  $8 \times 10^4$  4T1 cells/mL/well in 12-multiwell culture plates. When the cells were about 80% confluent, each well was injected with 1.85 KBq of  $^{177}\text{Lu}$ -DOTA-DG or 37 KBq of  $^{18}\text{F}$ -FDG in 1 mL of culture media. A blocking study was performed with the addition of 1 mg of 2-deoxy-D-glucose to cells (100 µL/well) treated with either  $^{177}\text{Lu}$ -DOTA-DG or  $^{18}\text{F}$ -FDG. After 4h of incubation at 37°C, the culture media were removed, and the cells were washed twice with PBS. The cells were then dissolved in 0.5% sodium dodecyl sulfate (0.5 mL/well). The radioactivity in the cells was measured using a gamma counter, using a radionuclide specific energy window, a counting time of 30s and a counting error  $\leq 5\%$ . The cell uptake of the radiotracer was calculated using the formula  $\% \text{uptake} = (\text{radioactivity of cells} / \text{total radioactivity}) \times 100\%$ .

### Murine breast cancer models

All animal studies were approved by the Southwest Medical University and were in compliance with the Laboratory Animal Regulations for the Care and Use of Animals. Female Kunming mice at 4–6 weeks of age were housed under specific pathogen-free conditions and kept on twelve-hour light and dark cycles in the Sichuan Key Laboratory of Nuclear Medicine and Molecular Imaging. To generate the breast cancer model, mice were implanted subcutaneously with  $2 \times 10^6$  4T1 cells in a 1:1 mixture of Matrigel (Corning, USA) on the right thighs. Mice were imaged and used in whole body biodistribution studies 15–20 days after implantation when the tumor grew to reach 8–10 mm in diameter.

### Whole body biodistribution of $^{177}\text{Lu}$ -DOTA-DG in tumor mice

Fifteen mammary tumor mice were divided to five groups with three mice in each group. They were anesthetized by 2% isoflurane inhalation and injected intravenously through caudal vein with  $^{177}\text{Lu}$ -DOTA-DG (3.7 MBq/mouse). Each group was euthanized by  $\text{CO}_2$  inhalation at five different time points, namely at 10min, 30min, 1h, 4h, 24h after injection. Blood was promptly withdrawn, and other organs such as heart, liver, spleen, kidney, muscle, tumor tissues etc were harvested. The weight of each organ/tissue was determined. The radioactivity was also measured using a gamma counter. Uptake of radiotracer in various organs/tissues was normalized to percentage injected dose per gram (% ID/g).

### Imaging of tumor mice with $^{177}\text{Lu}$ -DOTA-DG

Imaging studies were carried out on a dual-head gamma unit (Millennium VG5, GE Healthcare) equipped with a parallel-hole, low-energy collimator. Each tumor bearing mouse was injected via the tail vein with 0.1 mL of  $^{177}\text{Lu}$ -DOTA-DG (7.4 MBq). After injection, images were taken at 60min list-mode acquisition under anesthesia, with five mice in each group. The region of interest (ROI) was identified to be the area between tumor tissue and the contralateral thigh muscle, which was used to determine tumor-to-background ratios (T/NT).

### Comet assay

The comet assay was performed by adopting the protocol of OxiSelect™ Comet Assay Kit (Cell Biolabs, INC.). MCF-7 cells (breast adenocarcinoma cells) were purchased from the National Key Laboratory for Biological Treatment, West China Hospital, Sichuan University. All cells were maintained in Dulbecco's modified eagle's medium (Gibco, USA) supplemented with 10% fetal bovine serum penicillin-streptomycin 1% (v/v) (Gibco, USA). The cells were cultured in 5%  $\text{CO}_2$  incubator at 37°C in a humidified atmosphere. Cells were seeded in 6-well tissue-culture plates and incubated for 24h for adherence. Subsequently, cells were divided into three groups and each group was treated with  $^{177}\text{Lu}$ -DOTA-DG 3.7 MBq/well,  $^{177}\text{LuCl}_3$  3.7 MBq/well and DOTA-DG diluted to the same concentration of  $^{177}\text{Lu}$ -DOTA-DG as control group, for 24h, respectively [32]. All cells were harvested by trypsin digestion, washed with PBS and centrifuged. The supernatant was discarded and the cells were resuspended at  $1 \times 10^5$  cells/mL in ice-cold PBS. Seventy five µL of Comet Agarose per well was added onto the OxiSelect™ Comet Slide to create a Base Layer, in the dark at 4°C for 15 minutes. The resuspended cells were mixed with Comet Agarose at 1:10 ratio (v/v), and 75 µL/well of cells were immediately transferred onto the top of the Comet Agarose Base Layer, in the dark at 4°C for 15 minutes. The slide was transferred to a horizontal electrophoresis chamber, and was allowed to run for 20min at 25V and 300mA. Subsequently, the slides were rinsed with pre-chilled distilled water (~25 mL/slide) and this procedure was repeated twice every 2min. The final water rinse was aspirated and replaced with cold 70% ethanol for 5min. After the slides were completely dried, 100 µL/well of diluted Vista Green DNA Dye was added, and the slides were incubated at room temperature for 15min. The slides were viewed by epifluorescence microscopy using a FITC filter at a magnification of 10X (Carl Zeiss Apo Tome, Germany). A hundred of randomly selected cells were analyzed. The damaged DNA (containing cleavage and strand breaks) migrated further than intact DNA and produced a "comet tail" shape. The captured images were analyzed using Comet Score image analysis software, and the percentage of tail DNA content (% tail DNA) was measured as an indicator of DNA damage (single strand breaks).

### Statistical analysis

All data were expressed as mean  $\pm$  standard deviation (SD). Statistical analysis was carried out using the unpaired, 2-tailed

Student t test of variance with Microsoft Office (Excel) 365 or GraphPad Prism V.5.0. P value of less than 0.05 was considered statistically significant. The following marks are used throughout the paper: \*,  $P < 0.05$ ; \*\*,  $P < 0.01$ ; \*\*\*,  $P < 0.001$ .

## Results and Discussion

### DOTA-DG synthesis

We prepared DOTA-DG via an amide bond formation between DG and DOTA-NHS ester (Figure 1). The crude product was purified via semi-preparative HPLC column, which showed a retention time of 7.61 min with greater than 90% DOTA-DG purity. The mass/charge ratio ( $m/z$ ) of 566 for  $[M+H]^+$  was detected by electrospray ionization (ESI) mass spectrometry which is consistent with the calculated value for  $C_{22}H_{39}N_5O_{12}$  of 565.

The efficient synthesis of DOTA-DG sets the stage for the following radiolabeling step. As a versatile radiolabeling precursor, DOTA-DG was shown in literature to exhibit pro-neoplastic properties [33–34] and we predicted that it can be specifically taken up by tumor cells after chelation with  $^{177}\text{Lu}$  to  $^{177}\text{Lu}$ -DOTA-DG.

### Radiochemistry of $^{177}\text{Lu}$ -DOTA-DG

The reaction parameters for the radiosynthesis of  $^{177}\text{Lu}$ -DOTA-DG were investigated. Firstly, the radiolabeling reaction was screened at 25°C, 40°C, 60°C and 90°C. As shown in Figure 2, it is observed that the reaction proceeded at higher rates with increasing reaction temperatures. The radiochemical yield reached >98% in 30min when the reaction was performed at 90°C. In comparison, the reaction proceeded at a much slower rate at 25°C where 81% of radiochemical yield was obtained in 30min. It is noted that extended reaction time from 30min to 2h at lower temperatures, i.e., 25°C, 40°C and 60°C did not significantly improve the yield. Therefore, 90°C was determined to be the optimal temperature for radiolabeling.

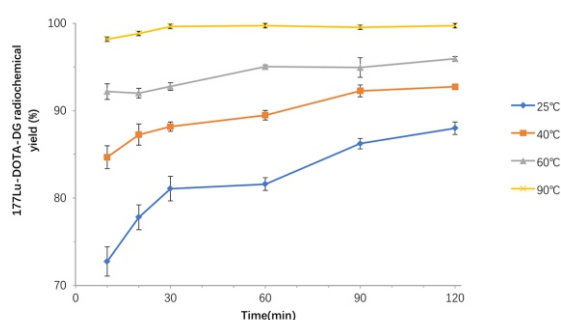


**Figure 2.** Dependence of the rate of  $^{177}\text{Lu}$ -DOTA-DG formation on temperature (pH=6, DOTA-DG =  $4 \times 10^{-3}\text{M}$ ,  $^{177}\text{Lu}$  = 3.7MBq).

Subsequently, we optimized the pH for the labeling of DOTA-DG with  $^{177}\text{Lu}$ . As shown in Figure 3, the optimal pH window for the reaction was determined to be 4.5 to 7. In the optimal pH window, the radiolabeled product was consistently obtained with greater than 95% yield in 30min. In contrast, the reaction was less efficient when conducted in pH of

2.5, 3.5, or 7.5. For instance, when the reaction was performed at the pH of 2.5, the radiochemical yield dropped drastically and less than 50% of radiolabeled product was obtained in 60min. Additionally, we studied the effects of the ligand concentration on the outcome of the radiolabeling reaction. As indicated in Figure 4, the optimal ratio for DOTA-DG precursor to  $^{177}\text{Lu}^{3+}$  was  $4 \times 10^{-4}\text{M}$  to  $^{177}\text{Lu}$  3.7MBq. Therefore, we identified the optimized reaction conditions for further experiments as follows: reaction time is 30min, reaction temperature is 90°C, pH=4.5 and DOTA-DG concentration is  $4 \times 10^{-4}\text{M}$  with respect to 3.7MBq of  $^{177}\text{Lu}^{3+}$ . The typical radiochromatogram of  $^{177}\text{Lu}$ -DOTA-DG at the optimized condition is shown in Figure 5. By taking advantage of the synthetic versatility of DOTA-DG, we envision a series of metal based radio-pharmaceutical agent can be prepared in a similar fashion as described above, thus greatly expanding our capability to develop novel radiopharmaceutical agents for cancer diagnosis and treatment [35].

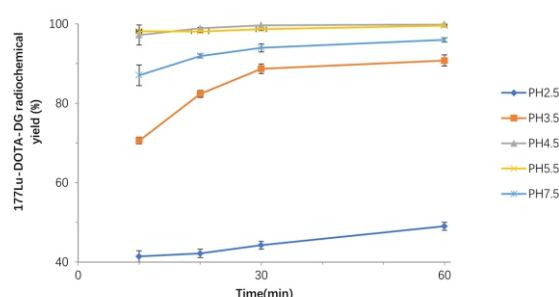


**Figure 3.** Dependence of the rate of  $^{177}\text{Lu}$ -DOTA-DG formation on pH (Temperature=90°C, DOTA-DG =  $4 \times 10^{-3}\text{M}$ ,  $^{177}\text{Lu}$  = 3.7MBq).

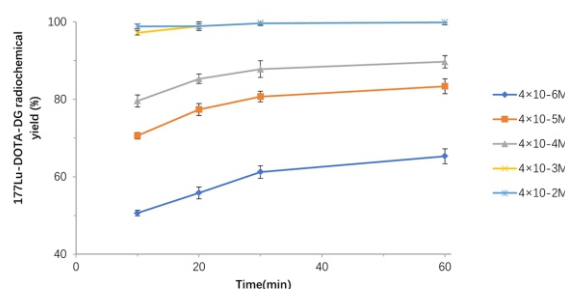


**Figure 4.** Dependence of the rate of  $^{177}\text{Lu}$ -DOTA-DG formation on ligand concentration (Temperature=90°C, pH=4.5,  $^{177}\text{Lu}^{3+}$  = 3.7MBq).

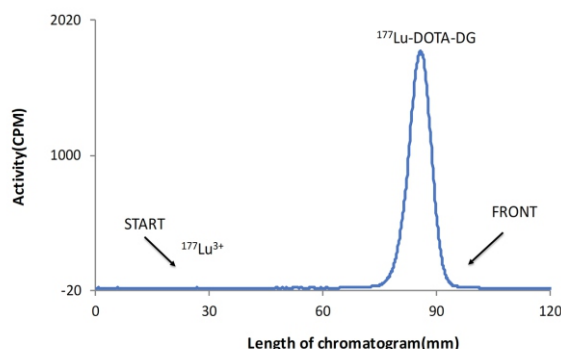


**Figure 5.** An example of radioTLC chromatogram of  $^{177}\text{Lu}$ -DOTA-DG, mobile phase: 10% ammonium acetate and 50% methanol mixture solution, pH=5.5.



### Stability of $^{177}\text{Lu}$ -DOTA-DG

The stability of the radiolabeled product in human blood serum and in PBS at 4h, 24h, 48h, 72h, 96h and 120h at 37°C were summarized in Figure 6. At 72h, 97% and 89% of the radiolabeled product remained intact in PBS and human blood serum, respectively. Further, 95% stability was observed for the control group where  $^{177}\text{Lu}$ -DOTA-DG was kept at room temperature in the original solution. As shown in Figure 6,  $^{177}\text{Lu}$ -DOTA-DG showed good stability up to 120h without significant radiolysis observed during this period of time. On average,  $94\pm0.53\%$ ,  $93\pm1.1\%$  and  $82\pm1.8\%$  of the radiolabeled product remained intact at 120h in the original solution, in PBS, and in human blood serum, respectively. The plasma metabolism is considered to be the major contributor of the lower stability observed in human blood serum. Nevertheless, the stability of  $^{177}\text{Lu}$ -DOTA-DG is over 80% up to 5 days in both PBS and human serum, indicating the feasibility of using  $^{177}\text{Lu}$ -DOTA-DG in clinical diagnostic and therapeutic applications.

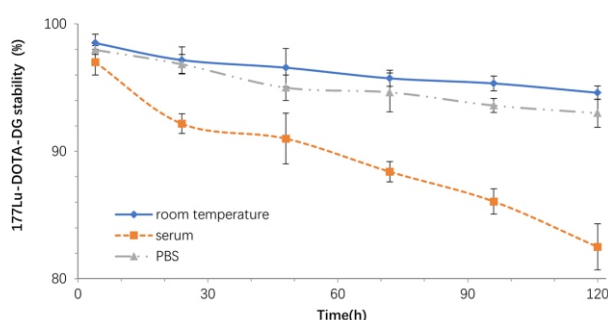


**Figure 6.** The stability of  $^{177}\text{Lu}$ -DOTA-DG at room temperature in PBS and human blood. Serum over the course of 120 h.

### In vitro cancer cell uptake

The cell uptake results for  $^{177}\text{Lu}$ -DOTA-DG and  $^{18}\text{F}$ -FDG in 4T1 cells after 4h of incubation is shown in Figure 7. The percentage cell uptake values for  $^{177}\text{Lu}$ -DOTA-DG and  $^{18}\text{F}$ -FDG were 4.64% and 10.34%, respectively. In order to investigate the binding specificity of  $^{177}\text{Lu}$ -DOTA-DG with glucose transporters, blocking experiments were carried out. When the cells were pre-treated with 1mg/mL of 2-deoxy-D-glucose (1mg/mL), the uptake value of  $^{18}\text{F}$ -FDG decreased significantly from 11% to 4% ( $P<0.001$ ). To our surprise, pre-treatment of deoxy-D-glucose did not block the uptake of  $^{177}\text{Lu}$ -DOTA-DG. As shown in the left two bars of Figure 7, no substantive change was observed for the cell uptake of  $^{177}\text{Lu}$ -DOTA-DG when the cells are pre-treated with 2-deoxy-D-glucose. These observations may be attributed to the non-specific binding of the  $^{177}\text{Lu}$ -DOTA-DG with tumor cells. Additionally, the blocking studies may also suggest  $^{177}\text{Lu}$ -DOTA-DG bind to receptors other than glucose transporters.

### Whole body biodistribution of $^{177}\text{Lu}$ -DOTA-DG in tumor mice

The data for whole body biodistribution of  $^{177}\text{Lu}$ -DOTA-DG was recorded at 5 different time points, namely, 10min,

30min, 60min, 4h and 24h after injection to mice bearing 4T1 tumors, and the results are summarized in Table 1. As shown in the first column of Table 1, a high initial kidney uptake was noted shortly after injection ( $t=10\text{min}$ ) which may due to kidney's function as a major urinary excretion pathway. At this time point, tumor tissues showed significant higher uptake (4.59%ID/g) of the  $^{177}\text{Lu}$ -DOTA-DG than all the other organs except for kidney. In comparison, low uptake was found in the brain, spleen, muscle, and intestines at the same time point ( $t=10\text{min}$ ). The tumor to muscle uptake ratios was calculated to be 5.68 at 10min after injection indicating high binding affinity with tumor tissues and excellent targeting selectivity of tumor over other organs. These advantageous features render  $^{177}\text{Lu}$ -DOTA-DG a promising imaging agent that generates high contrast images in clinics as well as an efficient radiotherapeutic agent that precisely delivers radiation to tumor cells without damaging healthy tissues. For direct comparison, the percentage injected dose in different organs at two representative time points (i.e., 10min and 30min) was summarized in Figure 8. Following the initial uptake, a rapid decrease of radioactivity was observed in several organs including tumor, lung, heart, bone, kidney, and blood. Particularly, a rapid washout of radioactivity from blood took place within 1h (10/60min ratio of 11.1). The radioactivity in intestines increased from 10min to 30min which is possibly attributed to the hepatobiliary elimination. It is worth noting that brain uptake remained low ( $<0.3\%\text{ID/g}$ ) throughout the time period after injection of the radiolabeled compound. This observation is consistent with the fact that blood-brain barrier plays an important role in regulating the compounds entering the central nervous system. Based on this result, we postulate that it is unlikely  $^{177}\text{Lu}$ -DOTA-DG will impose significant neurological toxicity issues for the diagnosis and treatment of cancer.

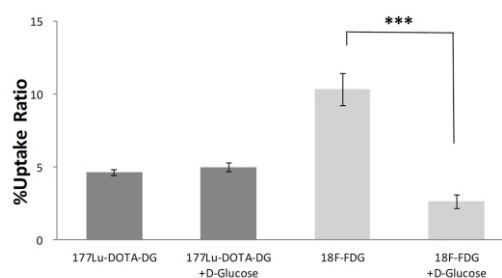


**Figure 7.** In vitro cellular uptake of  $^{177}\text{Lu}$ -DOTA-DG and  $^{18}\text{F}$ -FDG in 4T1 cells (in blocking experiments, both radiotracers were incubated with an excessive amount of D-glucose); \*\*\*:  $P<0.001$ .

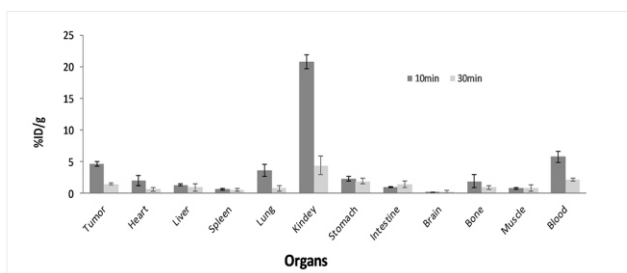


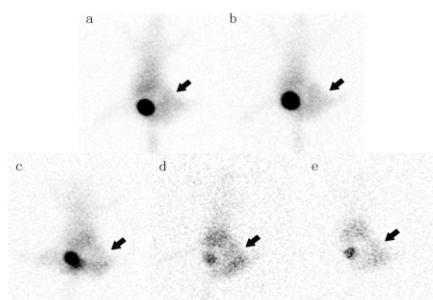
**Figure 8.** Whole body biodistribution of  $^{177}\text{Lu}$ -DOTA-DG (3.7MBq) at 10min and 30min in 4T1 tumor mice.

**Table 1.** Whole body biodistribution results of  $^{177}\text{Lu}$ -DOTA-DG in 4T1 tumor mice (Expressed as %ID/g $\pm$ SD, n=3).

Site	10min	30min	60min	4h	24h
Tumor	4.59 $\pm$ 0.36	1.47 $\pm$ 0.13	0.50 $\pm$ 0.05	0.10 $\pm$ 0.00	0.15 $\pm$ 0.03
Heart	1.99 $\pm$ 0.80	0.65 $\pm$ 0.29	0.19 $\pm$ 0.01	0.10 $\pm$ 0.10	0.08 $\pm$ 0.01
Liver	1.35 $\pm$ 0.19	0.96 $\pm$ 0.56	0.34 $\pm$ 0.03	0.12 $\pm$ 0.02	0.11 $\pm$ 0.03
Spleen	0.66 $\pm$ 0.14	0.55 $\pm$ 0.15	0.11 $\pm$ 0.03	0.12 $\pm$ 0.04	0.12 $\pm$ 0.03
Lung	3.62 $\pm$ 0.97	0.79 $\pm$ 0.45	0.52 $\pm$ 0.10	0.16 $\pm$ 0.02	0.14 $\pm$ 0.03
Kidney	20.74 $\pm$ 1.14	4.42 $\pm$ 1.43	2.26 $\pm$ 0.36	1.15 $\pm$ 0.26	0.52 $\pm$ 0.10
Stomach	2.24 $\pm$ 0.37	1.93 $\pm$ 0.44	1.26 $\pm$ 0.35	0.06 $\pm$ 0.01	0.07 $\pm$ 0.01
Intestine	0.99 $\pm$ 0.10	1.41 $\pm$ 0.49	0.24 $\pm$ 0.01	0.05 $\pm$ 0.01	0.05 $\pm$ 0.00
Brain	0.21 $\pm$ 0.03	0.28 $\pm$ 0.27	0.06 $\pm$ 0.03	0.05 $\pm$ 0.02	0.02 $\pm$ 0.00
Bone	1.91 $\pm$ 1.00	0.93 $\pm$ 0.31	0.74 $\pm$ 0.15	0.08 $\pm$ 0.04	0.08 $\pm$ 0.03
Muscle	0.81 $\pm$ 0.13	0.79 $\pm$ 0.52	0.20 $\pm$ 0.14	0.08 $\pm$ 0.01	0.03 $\pm$ 0.00
Blood	5.77 $\pm$ 0.84	2.14 $\pm$ 0.26	0.52 $\pm$ 0.11	0.02 $\pm$ 0.00	0.02 $\pm$ 0.00

Mean %ID/g ( $\pm$  standard deviation) **$^{177}\text{Lu}$ -DOTA-DG imaging of tumor mice**

The preliminary imaging results with  $^{177}\text{Lu}$ -DOTA-DG at five different time points are shown in Figure 9. In order to investigate tumor uptake and in vivo kinetics profile of the radiolabeled agent, we performed our study with 4T1 tumor mice. As shown in Figure 9(A), the tumor region was clearly visualized with high contrast to the background throughout the time period after injection. The distribution of the radiolabeled agent was heterogeneous, with the majority of the activity in tumor tissues. The uptake peaked at 30min and the in vivo kinetics profile obtained from  $^{177}\text{Lu}$ -DOTA-DG imaging studies is consistent with the ex vivo whole body biodistribution data. It is interesting to note that the region of interest (ROI) ratios for the tumor to non-tumor (T/NT ratios) gradually increased over the time (except for t=120 min). The T/NT ratio was calculated as 2.9, 3.6, 3.8, 4.3 and 2.4 at 10min, 30min, 60min, 90min and 120min, respectively. This trend suggested that there was a slower washout rate in tumor tissues than that in other organs. The stronger association of the radiolabeled compound with tumor tissues is beneficial for radionuclide therapy as it allows for longer exposure of tumor cells to radioactivity. It is worth noting that besides tumor tissues, kidneys, liver, and bladder were also visualized in the imaging study, albeit with less intensity.

**Figure 9.** Imaging of a 4T1 tumor bearing mouse acquired at 10min (a), 30min (b), 60min (c), 90min (d) and 120min (e) after injection of  $^{177}\text{Lu}$ -DOTA-DG (7.4MBq); arrows indicate the tumors. **$^{177}\text{Lu}$ -DOTA-DG radiation-Induced DNA damage**

In order to evaluate the potential mutagenic effect of  $^{177}\text{Lu}$ -DOTA-DG to induce DNA damage, Comet assays were carried out. As shown in Figure 10(A)-(C), cancer cells were exposed to  $^{177}\text{Lu}$ -DOTA-DG,  $^{177}\text{LuCl}_3$ , and blank control, respectively. By comparing the photomicrographs of stained DNA of MCF-7 cells in different groups, we observed cells treated with  $^{177}\text{Lu}$ -DOTA-DG showed longer and brighter tail which indicates a much higher degree of DNA damaging. Cells treated with  $^{177}\text{LuCl}_3$  showed shorter tails as compared to cells treated with  $^{177}\text{Lu}$ -DOTA-DG. In contrast, most non-treated cells remained in the cavity with a circle shape and no tail was observed, which indicated very low level of DNA damaging in these cells in the given time window. A total of 100 nucleoids were further analyzed for each group to determine the percentage of DNA in tail. As shown in Figure 10(D), cells treated with  $^{177}\text{Lu}$ -DOTA-DG and  $^{177}\text{LuCl}_3$  both showed statistically significant higher ratio of DNA tailing than cells in the control group. Moreover, despite the well-known genotoxicity of  $^{177}\text{LuCl}_3$  [36],  $^{177}\text{Lu}$ -DOTA-DG outperformed  $^{177}\text{LuCl}_3$  by inducing a higher degree of DNA damage in cancer cells. The DNA damaging progresses through several stages, including programmed cell-cycle delays, DNA single-strand breaks, and DNA double-strand breaks, cell death or DNA repair. The main damage induced by radiation occurs in the nucleus of cells [37]. In the Comet assay, we were able to quantify and distinguish cells with different rates of DNA damage, thus confirming a significant amount of DNA was damaged when the cells are exposed to  $^{177}\text{Lu}$ -DOTA-DG.

Summing the above, a novel  $^{177}\text{Lu}$ -labeled radiopharmaceutical  $^{177}\text{Lu}$ -DOTA-DG was synthesized and evaluated for stability, tumor binding affinity, tumor binding specificity and ability to induce DNA damage in cancer cells. The synthetic procedures for the radiolabeling reaction were efficient and operationally simple. Under the optimized conditions,  $^{177}\text{Lu}$ -DOTA-DG was prepared from readily available precursor (DOTA-DG) in 30min at 90°C with more than 98%

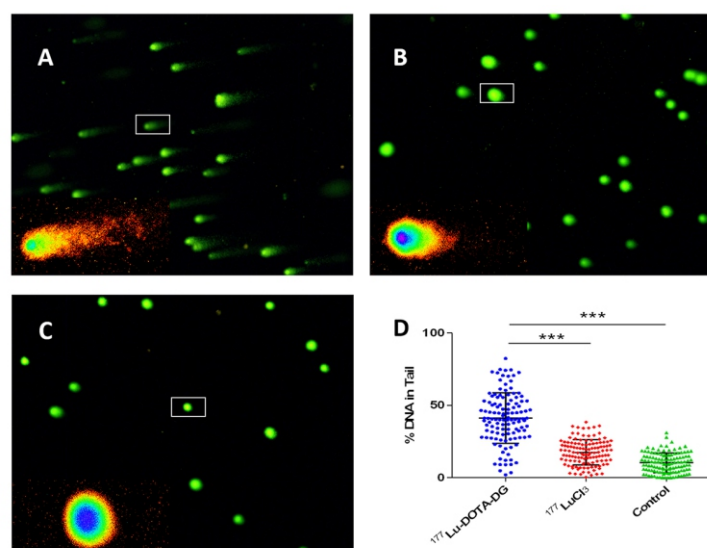


**Figure 10.** Photomicrographs of stained DNA of MCF-7 cells for alkaline comet as-say: (A) cells treated with  $^{177}\text{Lu}$ -DOTA-DG (3.7MBq) 24h; (B) cells treated with  $^{177}\text{LuCl}_3$  (3.7MBq) 24h; (C) non-treated cell; (D) a total of 100 nucleoids were analyzed for each group to obtain % DNA in tail; significant differences between  $^{177}\text{Lu}$ -DOTA-DG and  $^{177}\text{Lu}$ -DOTA and control cells (\*\*\* $P < 0.001$ ); the inset boxes in upper panels are shown at pseudorandom of single cell in lower panels.

radiochemical yield. The stability of  $^{177}\text{Lu}$ -DOTA-DG was evaluated in both PBS and human blood serum and high degree of stability (>80%) was noted up to 5 days. Preliminary in vitro cancer cells uptake and blocking experiments shed light on the non-specific binding of  $^{177}\text{Lu}$ -DOTA-DG with glucose transporters. Both whole body biodistribution studies and in vivo imaging studies demonstrated excellent tumor cells uptake, selective binding to tumor tissues, and favorable kinetics profile for following pre-clinical and clinical studies. Furthermore, the DNA damaging induced by  $^{177}\text{Lu}$ -DOTA-DG was confirmed by the Comet assays.

*In conclusion*, the present study presents a novel  $^{177}\text{Lu}$ -labeled agent which showed promising properties of targeting cancer tissues and inducing DNA damaging in mice. This study further suggests an alternative method for targeted radionuclide therapy. Further exploration of other chelation ligands/metal radionuclides and continued investigation to address non-specific binding issues are underway in our laboratory.

*The authors declare that they have no conflicts of interest.*

#### Author contributions

Jie Zhang designed and conducted most of the experiments. Zi Wang and Huipan Liu helped with data collection and initial phase improvement. Liang Cai helped with model building by 4T1 tumor implantation. Yue Feng and Hongyuan Wei helped for the synthesis and labeling of DOTA-DG. Jie Zhang and Zi Wang, Ying Xie, Yue Chen wrote the manuscript. Yue Chen and Ying Xie supervised the project.

#### Acknowledgements

This work was financially supported by the Foundation of Sichuan Key Laboratory of Nuclear Medicine and Molecular Imaging (2018JPT0023), Science and Technology Department of Sichuan province. We thank China Academy of En-

gineering Physics for kindly providing  $^{177}\text{Lu}$  radionuclide. We thank Professor Shaozhi Fu (Oncology Department, The Affiliated Hospital, Southwest Medical University) for kindly providing 4T1 murine breast cancer cells.

#### Bibliography

1. Speer TW. *Targeted radionuclide therapy*. Lippincott Williams & Wilkins; 2012.
2. Ersahin D, Doddamani I, Cheng D. Targeted radionuclide therapy. *Cancers* 2011; 3(4): 3838-55.
3. Dearnaley DP, Khoo VS, Norman AR et al. Comparison of radiation side-effects of conformal and conventional radiotherapy in prostate cancer: a randomised trial. *The Lancet* 1999; 353(9149): 267-72.
4. Zachariah B, Balducci L, Venkattaramanabala G, et al. Radiotherapy for cancer patients aged 80 and older: a study of effectiveness and side effects. *Int J Radiat Oncol Biol Phys* 1997; 39(5): 1125-9.
5. Lindley C, McCune JS, Thomason TE et al. Perception of chemotherapy side effects cancer versus noncancer patients. *Cancer Pract* 1999; 7(2): 59-65.
6. Uribe CF, Esquinas PL, Tanguay J et al. Accuracy of  $^{177}\text{Lu}$  activity quantification in SPECT imaging: a phantom study. *EJNMMI Phys* 2017; 4(1): 2.
7. Beauregard J-M, Hofman MS, Pereira JM et al. Quantitative  $^{177}\text{Lu}$  SPECT (QSPECT) imaging using a commercially available SPECT/CT system. *Cancer Imag* 2011; 11(1): 56.
8. Shcherbinin S, Piwowarska-Bilska H, Celler A, Birkenfeld B. Quantitative SPECT/CT reconstruction for  $^{177}\text{Lu}$  and  $^{177}\text{Lu}/^{90}\text{Y}$  targeted radionuclide therapies. *Phys Med & Biol* 2012; 57(18): 5733.
9. Jødal L. Beta emitters and radiation protection. *Acta Oncologica* 2009; 48(2): 308-13.
10. Gains JE, Bomanji JB, Fersht NL et al.  $^{177}\text{Lu}$ -DOTATATE molecular radiotherapy for childhood neuroblastoma. *J Nucl Med* 2011; 52(7): 1041.
11. Chakraborty S, Das T, Sarma HD et al. Comparative studies of  $^{177}\text{Lu}$ -EDTMP and  $^{177}\text{Lu}$ -DOTMP as potential agents for palliative radiotherapy of bone metastasis. *Appl Radiat Isot* 2008; 66(9): 1196-205.
12. Papamichail DG, Exadaktylou PE, Chatzipavlidou VD. Neuroendocrine tumors: Peptide receptors radionuclide therapy (PRRT). *Hell J Nucl Med* 2016; 19(1): 75-82.
13. Gerasimou G, Moralidis E, Gotzamani-Psarrakou A. Somatostatin receptor imaging with  $^{111}\text{In}$ -pentetate in gastro-intestinal tract and lung neuroendocrine tumors-Impact on targeted treatment. *Hell J Nucl Med* 2010; 13(2): 158-62.



14. Cheal SM, Xu H, Guo H-f et al. Theranostic pretargeted radioimmunotherapy of colorectal cancer xenografts in mice using picomolar affinity  $^{86}\text{Y}$ - or  $^{177}\text{Lu}$ -DOTA-Bn binding scFv C825/GPA33 IgG bispecific immunoconjugates. *Eur J Nucl Med Mol Imaging* 2016; 43(5): 925-37.
15. Emmett L, Willowson K, Violet J et al. Lutetium 177 PSMA radionuclide therapy for men with prostate cancer: a review of the current literature and discussion of practical aspects of therapy. *J Med Rad Sci* 2017; 64(1): 52-60.
16. Miao Y, Quinn TP. Peptide-targeted radionuclide therapy for melanoma. *Crit Rev Oncol Hematol* 2008; 67(3): 213-28.
17. Banerjee S, Pillai M, Knapp F. Lutetium-177 therapeutic radiopharmaceuticals: linking chemistry, radiochemistry, and practical applications. *Chem Rev* 2015; 115(8): 2934-74.
18. Pillai AM, Russ Knapp FF. Evolving important role of lutetium-177 for therapeutic nuclear medicine. *Curr Radiopharm* 2015; 8(2): 78-85.
19. Tagawa ST, Milowsky MI, Morris M et al. Phase II study of lutetium-177-labeled anti-prostate-specific membrane antigen monoclonal antibody J591 for metastatic castration-resistant prostate cancer. *Clin Cancer Res* 2013; 19(18): 5182-91.
20. Zaknun JJ, Bodei L, Mueller-Brand J et al. The joint IAEA, EANM, and SNMMI practical guidance on peptide receptor radionuclide therapy (PRRT) in neuroendocrine tumours. *Eur J Nucl Med Mol Imaging* 2013; 40(5): 800-16.
21. Schoffelen R, Boerman OC, Goldenberg DM et al. Development of an imaging-guided CEA-pretargeted radionuclide treatment of advanced colorectal cancer: first clinical results. *Br J Cancer* 2013; 109(4): 934.
22. Ilan E, Sandstrom M, Wassberg C et al. Dose response of pancreatic neuroendocrine tumors treated with peptide receptor radionuclide therapy using  $^{177}\text{Lu}$ -DOTATATE. *J Nucl Med* 2015; 56(2): 177-82.
23. Macheda ML, Rogers S, Best JD. Molecular and cellular regulation of glucose transporter (GLUT) proteins in cancer. *J Cell Physiol* 2005; 202(3): 654-62.
24. Fowler JS, Ido T. Initial and subsequent approach for the synthesis of  $^{18}\text{F}$ -FDG. *Semin Nucl Med* 2002; 32(1): 6-12.
25. Groeux D, Mankoff D, Espié M, Hindié E.  $^{18}\text{F}$ -FDG PET/CT in the early prediction of pathological response in aggressive subtypes of breast cancer: review of the literature and recommendations for use in clinical trials. *Eur J Nucl Med Mol Imaging* 2016; 43(5): 983-93.
26. Tripathi M, Tripathi M, Damle N et al. Differential diagnosis of neurodegenerative dementias using metabolic phenotypes on F-18 FDG PET/CT. *Neuroradiol J* 2014; 27(1): 13-21.
27. Krishnan HS, Ma L, Vasdev N, Liang SH.  $^{18}\text{F}$ -Labeling of Sensitive Biomolecules for Positron Emission Tomography. *Chem Eur J* 2017; 23(62): 15553-77.
28. Wei X, Liu Z, Zhao Z.  $^{68}\text{Ga}$  tagged dendrimers for molecular tumor imaging in animals. *Helv J Nucl Med* 2019; 22(1): 78-9.
29. Bertagna F, Giubbini R, Savelli G et al. A patient with medullary thyroid carcinoma and right ventricular cardiac metastasis treated by  $^{90}\text{Y}$ -Dotatoc. *Helv J Nucl Med* 2009; 12(2): 161-4.
30. Lee JY, Lee S-Y, Kim GG et al. Development of  $^{68}\text{Ga}$ -SCN-DOTA-Capsaicin as an Imaging Agent Targeting Apoptosis and Cell Cycle Arrest in Breast Cancer. *Cancer Bioth Radiopharm* 2017; 32(5): 169-75.
31. Chen Y, Huang ZW, He L et al. Synthesis and evaluation of a technetium-99m-labeled diethylenetriaminepentaacetate-deoxyglucose complex ( $^{99\text{m}}\text{Tc}$ -DTPA-DG) as a potential imaging modality for tumors. *Appl Radiat Isot* 2006; 64(3): 342-7.
32. Ping KY, Darah I, Chen Y, Sasidharan S. Cytotoxicity and genotoxicity assessment of *Euphorbia hirta* in MCF-7 cell line model using comet assay. *Asian Pac J Trop Biomed* 2013; 3(9): 692.
33. Yang Z, Zhu H, Lin X-f. Synthesis and evaluation of  $^{111}\text{In}$ -labeled D-glucose as a potential SPECT imaging agent. *J Radioanal Nucl Chem* 2013; 295(2): 1371-5.
34. Petrie V, Tishchenko V, Krasikova R.  $^{18}\text{F}$ -FDG and Other Labeled Glucose Derivatives for Use in Radionuclide Diagnosis of Oncological Diseases. *Pharm Chem J* 2016; 50(4): 209-20.
35. Burki TK.  $^{177}\text{Lu}$ -Dotatate for midgut neuroendocrine tumours. *The Lancet Oncol* 2017; 18(2): e74.
36. Kumar C, Korde A, Kumari K et al. Cellular toxicity and apoptosis studies in osteocarcinoma cells, a comparison of  $^{177}\text{Lu}$ -EDTMP and Lu-EDTMP. *Curr Radiopharm* 2013; 6(3): 146-51.
37. Bussink J, Span PN.  $\gamma$ -H2AX Foci in Peripheral Blood Lymphocytes to Quantify Radiation-Induced DNA Damage After  $^{177}\text{Lu}$ -DOTA-Octreotate Peptide Receptor Radionuclide Therapy. *J Nucl Med* 2015; 56(4): 501-2.



Édouard Manet (1832-1883). *A Bar at the Folies-Bergère* (1881/82). Oil in canvas. Courtauld Gallery, London.